J Mater Sci (2007) 42:6607–6613
DOI 10.1007/s10853-007-1528-7

# Prediction of residual stresses in welds of similar and dissimilar steel weldments

**Chin-Hyung Lee · Kyong-Ho Chang**

Received: 27 May 2006 / Accepted: 16 January 2007 / Published online: 2 May 2007


**Abstract** The fabrication of structural member using dissimilar steels renders steel structures lighter and more economical. However, it always involves welding process and produces different residual stresses in welds as compared with welding of similar steels. This paper presents the characteristics of residual stresses in welds of similar and dissimilar steel weldments by carrying out three-dimensional (3-D) thermal elastic-plastic finite element (FE) analysis. The materials used in this investigation were SM400, SM490, SM520 and SM570, widely used structural steels in welded structure. Results show that the maximum longitudinal residual stresses in welds of the similar steel weldments increase with increasing yield stress of the steel welded (SM400 < SM490 < SM520 < SM570). In case of the dissimilar steel weldments, the difference between the longitudinal residual stresses in welds increases with increasing yield stress of the steel welded together with SM400 (SM490 < SM520 < SM570).

## Introduction

As the spans of bridges are getting longer and the stories of buildings are getting higher, there are strong demands for high performance steel and high strength steel [1, 2]. Likewise, welding dissimilar steels renders steel structures lighter and more economical. The fabrication of structural member using dissimilar steels always involves welding process. Welding is a reliable and efficient metal joining process and widely used in construction, shipbuilding and steel bridges, etc. The advantage of welding as joining process includes high joint efficiency, simple set up and low fabrication cost. However, due to the localized heating during welding, complex thermal stresses are inevitably generated [3, 4].

Residual stresses that develop in and around the welded joint are detrimental to the integrity and the service behavior of the welded part. High residual tensile stresses in the region near the weld might promote failure by brittle fracture or may increase the susceptibility of a weld to fatigue damage, stress corrosion cracking during service. Residual tensile stresses also promote cold cracking in association with hydrogen in certain steels, even before the welded member is put in service [5]. Furthermore, welding of dissimilar steels produces different residual stresses in welds as compared with welding of similar steels. Therefore, it is very important to clarify characteristics of residual stresses in welds of similar and dissimilar steel weldments.

In this study, a 3-D thermal elastic-plastic FE analysis was conducted in order to investigate the characteristics of welding residual stresses, especially the longitudinal residual stresses which are most harmful to the integrity of the structure among the residual stress components, in welds of similar and dissimilar steel weldments.

## Theoretical background of the 3-D thermal elastic-plastic analysis

Complex numerical approaches are required to accurately model the welding process. In the analysis, one should

C.-H. Lee (✉)
Conventional Rail Engineering Corps, Korea Railroad Research Institute, 374-1, Woulam-dong, Uiwang-shi, Kyunggi-do 437-050, Korea
e-mail: ifinder@hanmail.net

K.-H. Chang
Department of Civil and Environmental Engineering, Chung-Ang University, 221, Huksuk-dong, Dongjak-ku, Seoul 156-756, Korea
e-mail: changkor@cau.ac.kr

account for: (1) conductive and convective heat transfer in the weld pool; (2) convective and radiative heat losses at the weld pool surface; (3) heat conduction into the surrounding solid materials as well as the conductive and convective heat transfer to ambient temperature [5]. Moreover, one needs to account for temperature-dependent material properties and the effects of liquid-to-solid and solid-state phase transformation in the materials [6].

The welding process is a coupled thermo-mechanical process. The thermal field strongly affects the residual stress field. On the other hand, the stress field has a weak influence on the thermal field. Therefore, uncoupled analysis works very well [7].

In this study, the thermo-mechanical behavior of the weldment during welding was simulated using an uncoupled 3-D thermo-mechanical FE formulation in order to accurately capture the temperature fields and the residual stresses in the weldment. The formulation consists of two stages and considers temperature-dependent thermo-physical and mechanical properties of the materials. First, the temperature distribution and its history in the welding model are computed by thermal analysis. The thermal analysis is based on the heat conduction formulation with the moving heat source. Then, the temperature history is employed as a thermal load in the subsequent mechanical analysis. The FE mesh and time steps for both the heat flow analysis and stress analysis are identical. The following subsections describe theoretical background of the FE formulation used for the present work.

## Thermal analysis

During welding the governing partial differential equation for the 3-D transient heat conduction, with internal heat generation and considering $\rho$, $K$ and $c$ as functions of temperature only, is given by the thermal equilibrium equation

$$\frac{\partial}{\partial x}\left(K(T)\frac{\partial T}{\partial x}\right)+\frac{\partial}{\partial y}\left(K(T)\frac{\partial T}{\partial y}\right)+\frac{\partial}{\partial z}\left(K(T)\frac{\partial T}{\partial z}\right)+Q = \rho(T)c(T)\frac{\partial T}{\partial t} \quad (1)$$

where $T$ is the temperature, $K$ is the thermal conductivity, $c$ is the specific heat, $\rho$ is the density and $Q$ is the rate of moving heat generation per unit volume.

The heat from the moving welding arc is applied as a volumetric heat source with a distributed heat flux (DFLUX) working on individual elements in the fusion zone (unit W/m$^3$). It is concerned to the specific weld parameters like voltage ($V$), current ($A$) and arc efficiency ($\eta$) by Eq. (2). The considered weld pool volume is denoted by $V_p$.

$$\mathrm{DFLUX} = \frac{V \cdot A \cdot \eta}{V_\mathrm{p}} \quad (2)$$

where $V_\mathrm{p}$ can be obtained by calculating the volume fraction of the elements in currently being welded zone. The arc efficiency factor is assumed as 0.85 for the FCA welding process used in the present analysis. The heat flux is applied during the time variation that corresponds to the approach and passing of the welding torch.

The heat exchange between the welded plate and its surroundings during welding and subsequent cooling takes place by both convection and radiation. This is modeled by defining the convection coefficient $h$, and emissivity $\varepsilon$ in the FE formulation. The heat flux losses on the surfaces of the welded plate due to the convection and radiation are given by

$$q_c = h(T - T_0)$$
$$q_r = \varepsilon\sigma(T^4 - T_0^4) \quad (3)$$

where $T_0$ = 20 °C is the room temperature; $\sigma = 5.67 \times 10^{-8}$ J/(m$^2$ K$^4$ s) is defined as the Stefan–Boltzmann constant. The convection coefficient is estimated using engineering formulae for natural convection to be 15 W/(m$^2$K) and the emissivity is defined to be $\varepsilon$ = 0.2 [5], respectively.

To account for the heat transfer due to fluid flow in the weld pool, an increase in thermal conductivity, which is several times larger than the value at room temperature, is assumed for the temperature above the melting temperature. However, liquid-to-solid phase transformation effects are not considered due to the lack of material information, especially at high temperatures, such as the near-melting state.

The weld filler variation with time is simulated by deactivating the elements in welded zone, which the welding torch has not yet approached, with zeroed stiffness. Then, the elements recover their stiffness depending on temperatures after the heat flux has passed them [8, 9].

## Mechanical (stress) analysis

The second step of the current analysis involves the use of the thermal histories predicted by the previous thermal analysis as an input (thermal loading) for the mechanical analysis. Welding-induced residual stresses are typical macro residual stresses and can be estimated using continuum mechanics.

*Displacement–strain relationship*

The strain of element can be written as follows

$$\{\varepsilon\} = \left\{\varepsilon_x\, \varepsilon_y\, \varepsilon_z\, \gamma_{yz}\, \gamma_{zx}\, \gamma_{xy}\right\}^T$$

$$\{\varepsilon\} = \{\varepsilon_O\} + \{\varepsilon_L\} \tag{4}$$

where $\{\varepsilon_O\}$ and $\{\varepsilon_L\}$ represent small strain and large strain, respectively, and given by

$$\{\varepsilon_O\} = \begin{Bmatrix} \varepsilon_x \\ \varepsilon_y \\ \varepsilon_z \\ \gamma_{yz} \\ \gamma_{zx} \\ \gamma_{xy} \end{Bmatrix} = \begin{Bmatrix} \partial u/\partial x \\ \partial v/\partial y \\ \partial w/\partial z \\ (\partial w/\partial y) + (\partial v/\partial z) \\ (\partial u/\partial z) + (\partial w/\partial x) \\ (\partial v/\partial x) + (\partial u/\partial y) \end{Bmatrix}$$

$$\{\varepsilon_L\} = \frac{1}{2}\begin{Bmatrix} \left(\frac{\partial u}{\partial x}\right)^2 + \left(\frac{\partial v}{\partial x}\right)^2 + \left(\frac{\partial w}{\partial x}\right)^2 \\ \left(\frac{\partial u}{\partial y}\right)^2 + \left(\frac{\partial v}{\partial y}\right)^2 + \left(\frac{\partial w}{\partial y}\right)^2 \\ \left(\frac{\partial u}{\partial z}\right)^2 + \left(\frac{\partial v}{\partial z}\right)^2 + \left(\frac{\partial w}{\partial z}\right)^2 \\ 2\left(\frac{\partial u}{\partial y}\frac{\partial u}{\partial z} + \frac{\partial v}{\partial y}\frac{\partial v}{\partial z} + \frac{\partial w}{\partial y}\frac{\partial w}{\partial z}\right) \\ 2\left(\frac{\partial u}{\partial z}\frac{\partial u}{\partial x} + \frac{\partial v}{\partial z}\frac{\partial v}{\partial x} + \frac{\partial w}{\partial z}\frac{\partial w}{\partial x}\right) \\ 2\left(\frac{\partial u}{\partial x}\frac{\partial u}{\partial y} + \frac{\partial v}{\partial x}\frac{\partial v}{\partial y} + \frac{\partial w}{\partial x}\frac{\partial w}{\partial y}\right) \end{Bmatrix}$$

It has been known that the incremental form of strain $\{d\varepsilon\}$ can be written as

$$\{d\varepsilon\} = [B]\{dw\} \tag{5}$$

where $[B]$ is the displacement-strain matrix.

*Stress–strain relationship*

The incremental form of stress–strain relation can be written as

$$\{\mathrm{d}\sigma\} = [D_d]\{\mathrm{d}\varepsilon\} - \{c\}\mathrm{d}T \tag{6}$$

where $[D_d]$ is divided into $[D_d^e]$ for the elastic range and $[D_d^p]$ for the plastic range, $\{c\}$ is a parameter to reflect the stress increment due to the dependence of the physical and mechanical properties of material on temperature.

*Equilibrium equation*

Applying the virtual work theorem to the equilibrium equation between nodal force and nodal displacement yields

$$\{\mathrm{d}F\} + \{L\} - \{\mathrm{d}R\} = [K]\{\mathrm{d}w\} \tag{7}$$

where $[K]$ is the element stiffness matrix, $\{\mathrm{d}F\}$ the increment of equivalent nodal force of element due to external force, $\{L\}$ the load correction term and $\{\mathrm{d}R\}$ the increment of equivalent nodal force of element due to temperature change.

Composing Eq. (7) for a whole structure and solving the linear simultaneous equations considering boundary conditions, the increment of nodal displacement $\{dw\}$ can be obtained. With the increment and using the displacement–strain relationship, the element strain can be obtained, thereby the element stress can be obtained using the constitutive law. The material is assumed to follow Von Mises yield criterion and the associated flow rules. Linear kinematic hardening rule is, also, assumed.

In the thermal and mechanical analyses, the effect of volume change due to the solid-state phase transformation (martensite transformation) on the residual stress is taken into account. The volume change is approximated by introducing modified specific heat and coefficient of thermal expansion. Details on the procedure can be found in the authors' work [6].

## Verification

In order to confirm the accuracy of the formulation used in this investigation, a specimen of butt joint welding of a thick-wall plate was constructed, with a length, width and thickness of $L = 500$ mm, $W = 500$ mm, $t = 30$ mm, respectively, as shown in Fig. 1. The joint was welded in the flat position with six passes using flux cored arc (FCA) welding process with SUPERCORED 81 electrode of 1.2 mm in diameter. The welding conditions and process parameters used in the fabrication of the joint are presented in Table 1 [6]. The base material is a high strength carbon

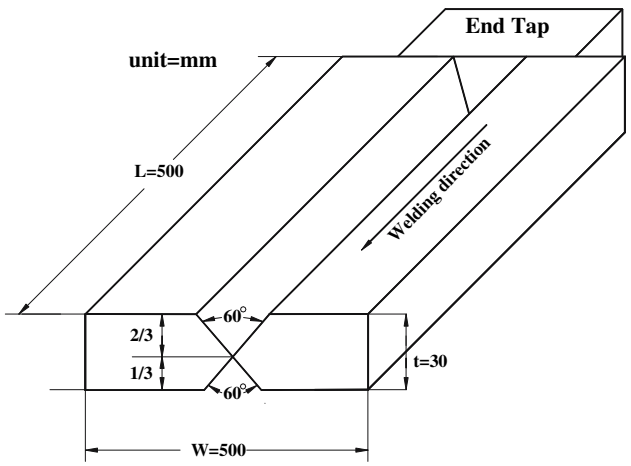


**Fig. 1** Joint configuration

**Table 1** Welding conditions and process parameters

| PASS | Current (A) | Voltage (V) | Speed (mm/s) |
|---|---|---|---|
| 1 | 250 | 30 | 3.1 |
| 2 | 270 | 32 | 2.9 |
| 3 | 280 | 35 | 2.0 |
| 4 | 280 | 35 | 2.4 |
| Turn Over | | | |
| 5 | 250 | 30 | 4.9 |
| 6 | 250 | 30 | 3.5 |

steel and Ref. [6] specifies the dependence of material properties on temperature. Therefore, these data are used for the residual stress analysis of the butt-welded joints.

The longitudinal residual stresses ($\sigma_x$) calculated by the FE model are compared to the experimental measurements which have been taken from the authors' work [6] as shown in Fig. 2. Residual stress measurements were carried out on the two-axis strain gauge with the saw cutting method. Gauges were intensively attached at welds of the specimen in order to investigate the residual stress relaxation due to phase transformation. Residual stresses were measured by calculating the difference between the initial strains and the residual strains after saw cutting. The results are normalized by the respective yield stress ($\sigma_{Y0}$) of the weld metal and base metal. Lower residual stresses in welds are attributed to the volumetric expansion due to the solid-state phase transformation. It shows that a good agreement is achieved in predicting the residual stresses that develop due to the welding process.

## Determination of residual stresses in welds of similar and dissimilar steel weldments

### FE model

FE thermal simulation of a butt joint welding process was carried out using the uncoupled thermo-mechanical formulation. Two 1,000 mm × 500 mm × 6 mm plates were assumed to be welded by one pass welding. The welded plate and the shape of groove are schematically shown in Fig. 3. The welding parameters chosen for this analysis were as follows: welding method, FCA welding process; welding current, 240 A; welding voltage, 30 V; and welding speed, 6 mm/s, respectively. A non uniform FE mesh with 8-noded isoparametric solid elements and four layers were used to discretize the computational domain. A fine mesh is used in the welding area in order to apply heat flux more accurately when the moving heat source passes the area at specific time steps. For the thermal model, only half of the plate may be used in order to expedite the runtime. Since the temperature distributions were found to be close to symmetric about the weld centerline by previous researchers, this is a reasonable approach for the sake of efficiency. However, in the mechanical model, such symmetry is interpreted as totally constrained displacement boundary conditions at the centerline plane of symmetry and leads to artificially high residual stresses [10]. Therefore, in this work, the whole plate is taken as analysis part in both thermal and mechanical analyses. In the mechanical model, the same FE mesh as in the thermal model was employed except for the applied boundary conditions. The movement of bottom plate was restrained to approximately model the actual welding conditions.

SM400, SM490, SM520 and SM570, one of the most widely used structural steels in Korea, have been used as the materials of choice. The chemical composition of the

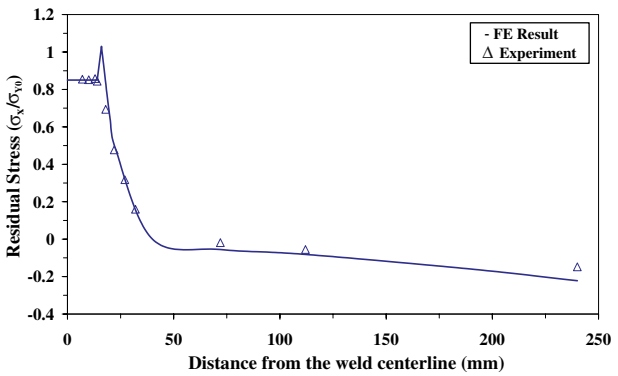


**Fig. 2** Comparison of the FE result with the experiment

| | A | B |
|---|---|---|
| Type1 | SM400 | SM490 |
| Type2 | SM400 | SM520 |
| Type3 | SM400 | SM570 |

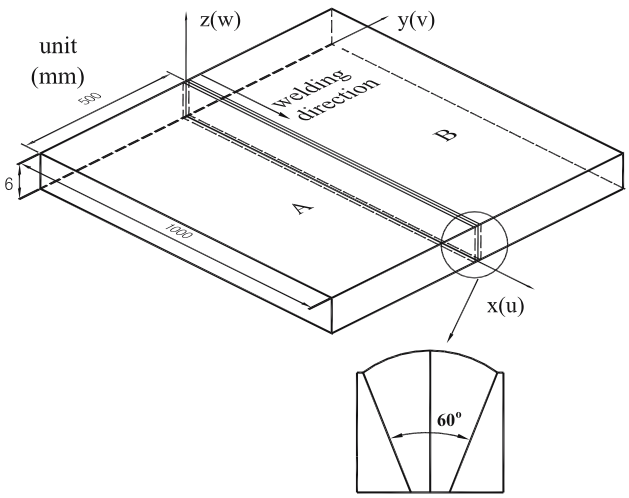


**Fig. 3** Dimensions of welded plate and shape of groove

**Table 2** Chemical composition of the materials used (mass, %)

| Materials | C | Si | Mn | P | S | Ni | Cr | Mo | Cu | V | Al | N |
|---|---|---|---|---|---|---|---|---|---|---|---|---|
| SM400 | 0.14 | 0.045 | 1.14 | 0.014 | 0.022 | 0.01 | 0.01 | 0.002 | 0.04 | 0.002 | 0.007 | 0.0049 |
| SM490 | 0.14 | 0.39 | 1.29 | 0.020 | 0.020 | 0.08 | 0.01 | 0.02 | 0.04 | 0.006 | 0.031 | 0.0065 |
| SM520 | 0.17 | 0.46 | 1.44 | 0.017 | 0.006 | 0.02 | 0.03 | – | 0.04 | – | 0.019 | 0.066 |
| SM570 | 0.15 | 0.45 | 1.38 | 0.013 | 0.007 | 0.02 | 0.02 | – | 0.11 | 0.068 | 0.021 | 0.004 |

materials is presented in Table 2. Furthermore, temperature-dependent thermo-physical properties such as thermal conductivity, specific heat and density, and temperature-dependent thermo-mechanical properties such as Young's modulus, thermal expansion coefficient and yield stress, are shown in Figs. 4 and 5, respectively [11–14].

For the weld metal, autogeneous weldment was assumed. This means that weld metal, HAZ and base metal share the same mechanical properties [9]. The width of welds was assumed to be the same as that of the heat source.

During the welding process, because the solid-state-phase transformation does not occur in the structural steels used in this work [15], the effect of volume change due to the phase transformation on the residual stress was not considered.

## Results and discussion

From the stress analysis all the stress and strain components can be obtainable. Here, we will discuss only the relevant data. In this discussion, three words ''longitudinal'', ''transverse'' and ''through-thickness'' are used to denote the residual stress components of three perpendicular directions. The word ''longitudinal'' is normally used for the welding direction and the word ''transverse'' is used for the direction perpendicular to the longitudinal (i.e. along the plate width), finally the word ''through-thickness (normal)'' is used for the direction perpendicular to the longitudinal and transverse (i.e. along the plate thickness).

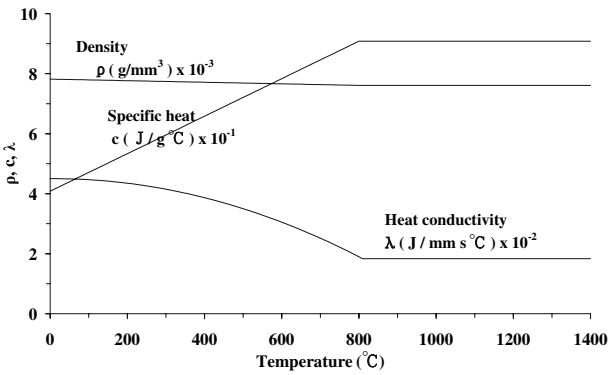


**Fig. 4** Temperature-dependent thermo-physical constants of the materials

Figure 6 shows the longitudinal, transverse and through-thickness (normal) residual stress profiles at a cross-section of the weldpiece perpendicular to the welding direction and half way through the weld length ($x$ = 500) when welding similar steels. Figure 6a–d show the results for the SM400, SM490, SM520 and SM570 weldment, respectively. The stress profiles are reported for depth at 1 mm from the upper surface. Highest tensile longitudinal residual stresses arise in welds due to the resistance of the material against contraction attributed to cooling after welding. The longitudinal residual stresses level out in compression away from the weld for self-equilibrating purpose. On the contrary, the transverse residual stresses are wholly tensile and level out to zero. The normal stress components have fluctuating profiles that vary between tensile and compressive. Results also reveal that the maximum longitudinal residual stresses increase (366 < 452 < 503 < 578 (MPa)) with increasing yield stress of the steel welded (SM400 < SM490 < SM520 < SM570). In general, welds

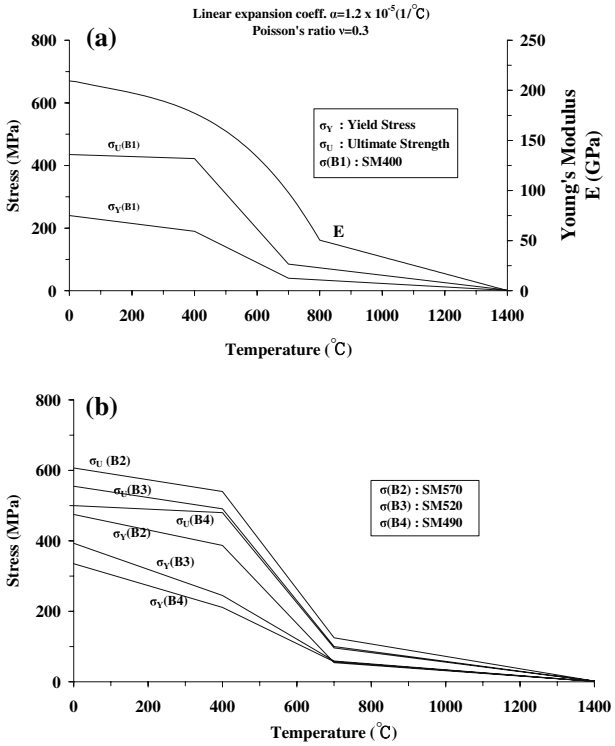


**Fig. 5** Temperature-dependent thermo-mechanical properties of the materials

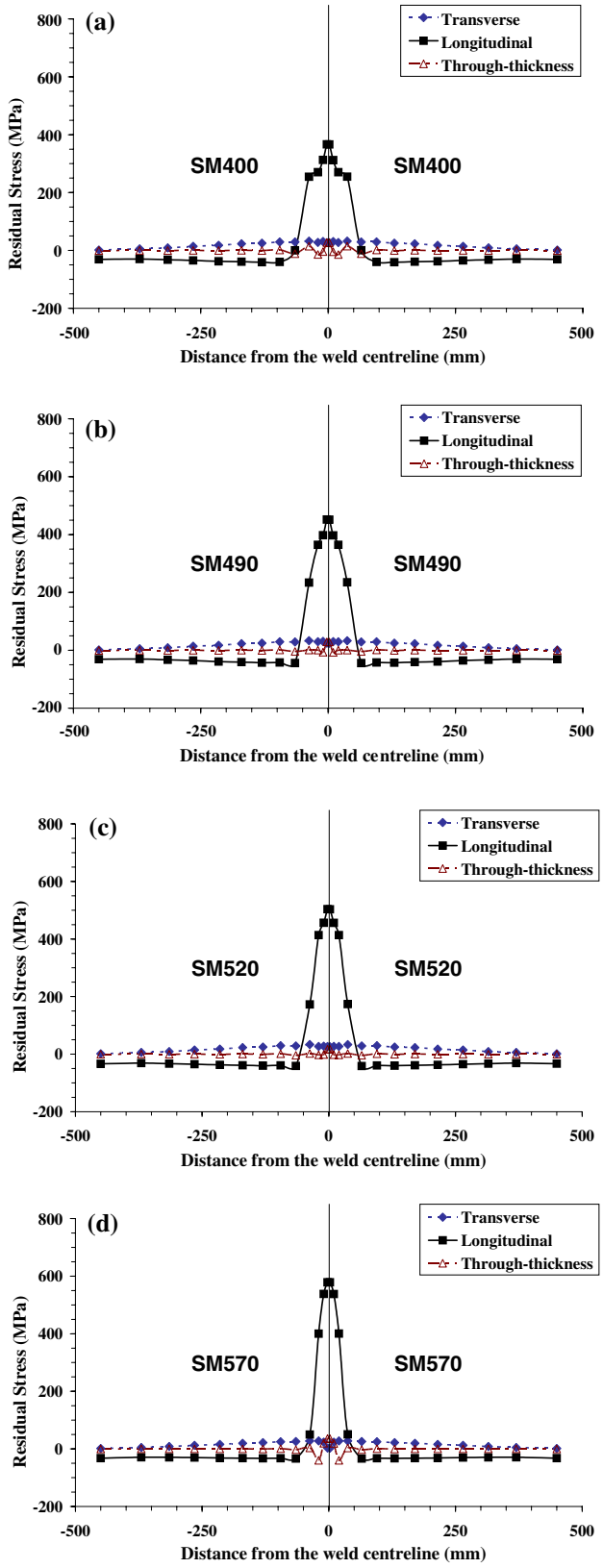


**Fig. 6** Residual stress profiles at a cross-section of the weldpiece perpendicular to the welding direction (Similar steels)

undergo yielding in the process of cooling after welding; then tensile residual stresses over yield stress of the weld, which are generated by the resistance of the material against contraction by cooling after welding, remain there. Hence, residual stresses in welds increase with increasing yield stress of the steel welded. The present analysis yielded similar results through the thickness, which are not presented here.

Figure 7 shows the residual stress profiles when welding dissimilar steels at the same locations as the similar steel weldments. Figure 7a shows the Type1 (SM400/SM490)

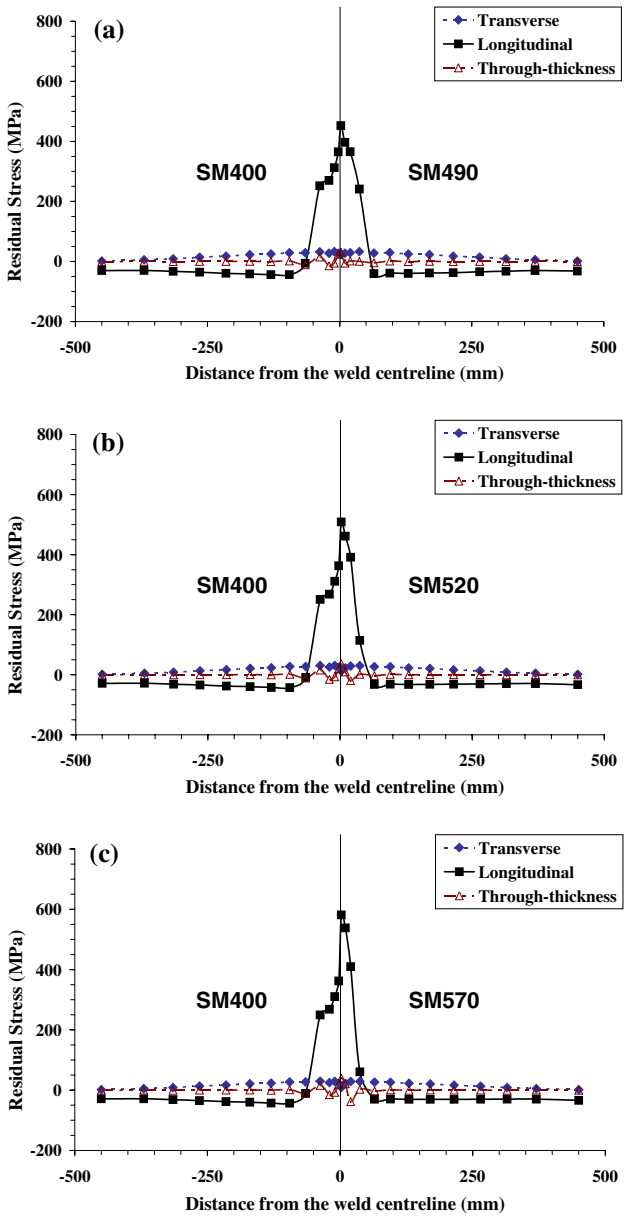


**Fig. 7** Residual stress profiles at a cross-section of the weldpiece perpendicular to the welding direction (Dissimilar steels)

welding result, which shows that the overall trends and shapes of the residual stress profiles are similar to those of the similar steel weldments but the longitudinal residual stresses in welds of SM400 are smaller than those in welds of SM490. This is because, explained above, the yield stress of SM490 is larger than that of SM400. Figure 7b shows the Type2 (SM400/SM520) welding result, which is similar to Type1. Nonetheless, the result shows that the difference between the longitudinal residual stresses in welds is larger (146 MPa) than Type1 (87 MPa). Figure 7c shows the Type3 (SM400/SM570) welding result, which is similar to Type1 and Type2. The result shows that the difference between the longitudinal residual stresses in welds is the largest (219 MPa) among the three Types. Similar results were shown through the thickness, which are not presented here.

## Conclusions

This study presents the characteristics of residual stresses in welds of similar and dissimilar steel weldments by carrying out 3-D thermal elastic-plastic FE analysis.

First, the temperature distribution and its history in the welding model were computed by thermal analysis. The thermal analysis was based on the heat conduction formulation with the moving heat source. Then, the temperature history was employed as a thermal load in the subsequent mechanical analysis. The FE mesh and time steps for both the heat flow analysis and stress analysis were identical. Based on the results in this work, the following conclusions can be made;

(a) The maximum longitudinal residual stresses in welds of the similar steel weldments increase with increasing yield stress of the steel welded (SM400 < SM490 < SM520 < SM570).
(b) The difference between the longitudinal residual stresses in welds of the dissimilar steel weldments increases with increasing yield stress of the steel welded together with SM400 (SM490 < SM520 < SM570).

## References

1. Miki C, Homma K, Tominaga T (2002) J Constr Steel Res 58:3
2. Bjorhovde R (2004) J Constr Steel Res 60:393
3. Murthy YVLN, Venkata Rao G, Krishna Layer P (1996) Comput Struct 60(1):131
4. Zhongqing Z, Peter FT, Lam YC, Daniel DWY (2003) J Mater Process Technol 132:184
5. Taljat B, Radhakrishnan B, Zacharia T (1998) Mater Sci Eng A 246:45
6. Chang KH, Lee CH (2006) Mater Trans 47(2):348
7. Askari A, Das S (2006) J Mater Process Technol 173(1):1
8. Brickstad B, Josefson BL (1998) Inter J Press Vessels Piping 75:11
9. Teng TL, Chang PH, Tseng WC (2003) Comput Struct 81:273
10. Khandkar MZH, Khan JA, Reynolds AP, Sutton MA (2006) J Mater Process Technol 174(1–3):195
11. Division of high temperature strength in JSSC Technical Committee (1968) In: The contents of mechanical properties of structural steels in high temperature and after heating.
12. Kim YC, Chang KH, Horikawa K (1999) Trans JWRI 27(1):69
13. Kim YC, Chang KH, Horikawa K (1999) Trans JWRI 27(2):107
14. Kim YC, Chang KH, Horikawa K (1999) In: Proceedings of the WTIA 46th International Conference. p. 1
15. Lee CH, Chang KH, Park HC, Lee JH (2006) J KSSC 18(3):395